

# The effects of reionization on $\text{Ly}\alpha$ galaxy surveys

Steven R. Furlanetto,<sup>1\*</sup> Matias Zaldarriaga,<sup>2,3</sup> & Lars Hernquist<sup>2</sup>

<sup>1</sup>*Division of Physics, Mathematics, & Astronomy; California Institute of Technology; Mail Code 130-33; Pasadena, CA 91125*

<sup>2</sup>*Harvard-Smithsonian Center for Astrophysics, 60 Garden St., Cambridge, MA 02138*

<sup>3</sup>*Jefferson Laboratory of Physics; Harvard University; Cambridge, MA 02138*

28 June 2018

## ABSTRACT

Searches for  $\text{Ly}\alpha$  emission lines are among the most effective ways to identify high-redshift galaxies. They are particularly interesting because they probe not only the galaxies themselves but also the ionization state of the intergalactic medium (IGM): nearby neutral gas efficiently absorbs  $\text{Ly}\alpha$  photons. The observed line strengths depend on the amount by which each photon is able to redshift away from line center before encountering neutral gas and hence on the size distribution of HII regions surrounding the sources. Here, we use an analytic model of that size distribution to study the effects of reionization on the luminosity function of  $\text{Ly}\alpha$ -emitters and their observed spatial distribution. Our model includes the clustering of high-redshift galaxies and thus contains ionized bubbles much larger than those expected around isolated galaxies. As a result,  $\text{Ly}\alpha$ -emitting galaxies remain visible earlier in reionization: we expect the number counts to decline by only a factor  $\sim 2$  (or 10) when the mean ionized fraction falls to  $\bar{x}_i \sim 0.75$  (or 0.5) in the simplest model. Moreover, the absorption is not uniform across the sky: galaxies remain visible only if they sit inside large bubbles, which become increasingly rare as  $\bar{x}_i$  decreases. Thus, the size distribution also affects the apparent clustering of  $\text{Ly}\alpha$ -selected galaxies. On large scales, it traces that of the large bubbles, which in our model are more biased than the galaxies. On small scales, the clustering increases rapidly as  $\bar{x}_i$  decreases because large HII regions surround strong galaxy overdensities, so a survey automatically selects only those galaxies with neighbours. The transition between these two regimes occurs at the characteristic bubble size. Hence, large  $\text{Ly}\alpha$  galaxy surveys have the potential to measure directly the size distribution of HII regions during reionization.

**Key words:** cosmology: theory – galaxies: evolution – intergalactic medium

## 1 INTRODUCTION

The reionization of hydrogen in the intergalactic medium (IGM) is a landmark event, because it defines the moment at which structure formation affected every baryon in the Universe. In the past few years, astronomers have made enormous strides in understanding this transition. The rapid onset of Gunn & Peterson (1965) absorption in the spectra of  $z > 6$  quasars (Becker et al. 2001; Fan et al. 2002; White et al. 2003) indicates that reionization probably ended at  $z \sim 6$  (albeit with large variance among different lines of sight: Wyithe & Loeb 2004a; Oh & Furlanetto 2005). On the other hand, the detection of a large optical depth to electron scattering for cosmic microwave background photons (Kogut et al. 2003) indicates (albeit with relatively low confidence) that the process began at  $z \gtrsim 15$ . Reionization thus appears to be a complex process, a conclusion strengthened by several other studies (Theuns et al. 2002; Wyithe & Loeb 2004b; Mesinger & Haiman 2004), so new methods to study the “twilight zone” of reionization are crucial.

One particularly intriguing technique is to search for  $\text{Ly}\alpha$ -

emitting galaxies in the high-redshift universe (e.g., Hu et al. 2002; Rhoads et al. 2004; Santos et al. 2004; Stanway et al. 2004; Taniguchi et al. 2005). These surveys offer a number of advantages. First, narrowband searches reduce the sky background, especially if placed between the bright sky lines that (nearly) blanket the near-infrared sky (e.g., Barton et al. 2004). Second, they efficiently select galaxies at a known redshift (although with some contamination by lower-redshift interlopers). Third, they increase the signal-to-noise by focusing on an emission line. Beyond these practical advantages, such surveys also constrain both the sources responsible for reionization (and in particular young massive stars; Partridge & Peebles 1967) and the ionization state of the IGM itself, because  $\text{Ly}\alpha$  photons will be absorbed if they pass through neutral gas near the galaxy. This is a consequence of the enormous  $\text{Ly}\alpha$  optical depth of a neutral IGM:  $\tau_{\text{GP}} \sim 6.5 \times 10^5 \bar{x}_{\text{HI}} [(1+z)/10]^{3/2}$  (Gunn & Peterson 1965), so even those photons passing through the damping wing of the  $\text{Ly}\alpha$  resonance will be absorbed (Miralda-Escudé 1998).

Thus, as the IGM becomes more neutral, the  $\text{Ly}\alpha$  selection technique will detect fewer and fewer objects (even after accounting for cosmological evolution in their intrinsic abundance); the

\* Email: sfurlane@tapir.caltech.edu

number of such galaxies therefore measures the globally averaged ionized fraction  $\bar{x}_i$  (Madau & Rees 2000; Haiman 2002; Santos 2004). Recently, Malhotra & Rhoads (2004) used these arguments to constrain the neutral fraction at  $z = 6.5$  (see also Stern et al. 2005). They compared luminosity functions of Ly $\alpha$ -emitters at  $z = 5.7$  and  $z = 6.5$  (bracketing the time at which quasar spectra indicate that reionization ends) and found no evolution in the number density over this range. By comparing to existing models of the Ly $\alpha$  damping wing absorption around isolated galaxies (Santos 2004), they concluded that this required  $\bar{x}_i \gtrsim 0.7$  at  $z = 6.5$ . Haiman & Cen (2005) reached a similar conclusion using different models (but the same luminosity function data).

The optical depth encountered by a galaxy's Ly $\alpha$  photons depends primarily on the extent of the HII region surrounding it: the photons redshift as they stream through the ionized gas (suffering little absorption), so they are somewhere in the wings of the line by the time they encounter the neutral gas. Thus, the amount of absorption depends sensitively on the size distribution of ionized bubbles during reionization. Existing analyses treat each galaxy in isolation (Santos 2004; Haiman & Cen 2005), so the HII regions are rather small even late in reionization. However, both analytic models (Barkana & Loeb 2004) and simulations (Ciardi et al. 2003; Sokasian et al. 2003, 2004) show that galaxies are highly clustered at these high redshifts. Furlanetto et al. (2004b, hereafter FZH04) developed an analytic model to calculate the size distribution of ionized bubbles around overdensities of sources. They showed that galaxy HII regions overlap quickly, growing much larger than expected in isolation (reaching scales of  $\gtrsim 10$  comoving Mpc when  $\bar{x}_i \gtrsim 0.65$ ). We describe this model in §2. Such large bubbles obviously reduce the damping wing absorption. Furlanetto et al. (2004a, hereafter FHZ04) showed that clustering therefore allows Ly $\alpha$  lines to be visible so long as the galaxy sits inside a relatively large bubble (see also Wyithe & Loeb 2005). In §3 we show that the large HII regions expected during reionization reduce the Ly $\alpha$  absorption for a given  $\bar{x}_i$ , and we compute the expected decline in the number counts of Ly $\alpha$ -selected galaxies throughout reionization.

Although this weakens the constraint on  $\bar{x}_i$  given by Malhotra & Rhoads (2004), it implies that the Ly $\alpha$  selection technique should remain viable deeper into reionization, making these surveys even more exciting. Moreover, the *distribution* of bubble sizes implies that the damping wing absorption is spatially variable: the bubbles essentially modulate the selection function of the survey. Thus, when large bubbles are rare (early in reionization), we expect to find isolated clumps of Ly $\alpha$ -emitting galaxies separated by apparent voids. We show in §4 that the bubbles affect the observed clustering pattern on both large and small scales: Ly $\alpha$ -selected galaxies will show a scale-dependent bias, with the magnitude depending on  $\bar{x}_i$  and a break appearing at the characteristic scale of the bubbles. We discuss the implications of these results in §5.

In our numerical calculations, we assume a cosmology with  $\Omega_m = 0.3$ ,  $\Omega_\Lambda = 0.7$ ,  $\Omega_b = 0.046$ ,  $H = 100h \text{ km s}^{-1} \text{ Mpc}^{-1}$  (with  $h = 0.7$ ),  $n = 1$ , and  $\sigma_8 = 0.9$ , consistent with the most recent measurements (Spergel et al. 2003). Unless otherwise specified, we quote distances in comoving units.

## 2 THE FZH04 MODEL

Recent numerical simulations (e.g., Ciardi et al. 2003; Sokasian et al. 2003, 2004) show that reionization proceeds

“inside-out” from high density clusters of sources to voids. We therefore associate HII regions with large-scale overdensities. We assume that a galaxy of total mass  $m_{\text{gal}}$  can ionize baryons associated with a total mass of  $\zeta m_{\text{gal}}$ , where  $\zeta$  is a constant that depends on (among other things) the efficiency of ionizing photon production, the escape fraction of these photons from the host galaxy, the star formation efficiency, and the mean number of recombinations. Each of these quantities is highly uncertain (e.g., massive Population III stars can dramatically increase the ionizing efficiency; Bromm et al. 2001), but at least to a rough approximation they can be collapsed into this single efficiency factor. The criterion for a region to be ionized by the galaxies contained inside it is then  $f_{\text{coll}} > \zeta^{-1}$ , where  $f_{\text{coll}}$  is the fraction of mass bound in haloes above some  $m_{\text{min}}$ . Unless otherwise specified, we will assume that  $m_{\text{min}} = m_4$ , corresponding to a virial temperature  $T_{\text{vir}} = 10^4 \text{ K}$  where hydrogen line cooling becomes efficient. In the extended Press-Schechter model (Lacey & Cole 1993), this places a condition on the mean overdensity within a region of mass  $m$ ,  $\delta > \delta_x(m, z)$ . FZH04 showed how to construct the mass function of HII regions from  $\delta_x$  in an analogous way to the halo mass function (Press & Schechter 1974; Bond et al. 1991). We first approximate the threshold  $\delta_x$  as  $\delta_x \approx B(m, z) \equiv B_0 + B_1 \sigma^2(m)$ , where  $\sigma^2(m)$  is the variance of density fluctuations on the scale  $m$ . This linear approximation turns out to be quite accurate. Then we can write the comoving number density of HII regions with masses in the range  $m \pm dm/2$  as (Sheth 1998; McQuinn et al. 2005):

$$n_b(m) dm = \sqrt{\frac{2}{\pi}} \frac{\bar{\rho}}{m^2} \left| \frac{d \ln \sigma}{d \ln m} \right| \frac{B_0(z)}{\sigma(m)} \times \exp \left[ -\frac{B^2(m, z)}{2\sigma^2(m)} \right] dm, \quad (1)$$

where  $\bar{\rho}$  is the mean density of the universe. FZH04 showed some examples of how the bubble sizes evolve throughout the early and middle stages of reionization. Several key properties of this model deserve emphasis. First, the bubbles are large: tens of comoving Mpc for  $\bar{x}_i \gtrsim 0.65$ . This is because high-redshift galaxies cluster strongly, so small mass overdensities translate to much larger overdensities of galaxies. There are other independent lines of evidence suggesting large HII regions during reionization (Wyithe & Loeb 2004a; Cen 2005). Furthermore, the bubbles attain a well-defined characteristic size  $R_c$  at any point during reionization. We show how  $R_c$  evolves in Figure 1a. The solid line is for  $z = 10$  and the long-dashed line is for  $z = 6.5$  with  $m_{\text{min}} = m_4$ . The other curves increase  $m_{\text{min}}$  at  $z = 6.5$ . Including only the massive galaxies increases the bias of the underlying galaxy population and hence makes the bubbles larger (Furlanetto et al. 2005a). Finally,  $n_b(m)$  is fairly robust to the underlying parameters of galaxy formation. For example, Figure 1a shows that  $R_c$  varies only weakly with  $z$  (or equivalently  $\zeta$ ) at a fixed  $\bar{x}_i$ .

By constructing  $n_b(m)$  and the halo mass function  $n_h(m)$  with the same formalism, the FZH04 model allows a straightforward connection between the two populations. For example, according to the extended Press-Schechter model the halo number density inside a bubble of mass  $m_b$  is (Lacey & Cole 1993; FZH04)

$$n_h(m_h | m_b) = \sqrt{\frac{2}{\pi}} \frac{\bar{\rho}}{m_h^2} \left| \frac{d \ln \sigma}{d \ln m_h} \right| \frac{\sigma^2(m_h) [\delta_c(z) - B(m_b)]}{[\sigma^2(m_h) - \sigma^2(m_b)]^{3/2}} \times \exp \left\{ -\frac{[\delta_c(z) - B(m_b)]^2}{2[\sigma^2(m_h) - \sigma^2(m_b)]} \right\}, \quad (2)$$

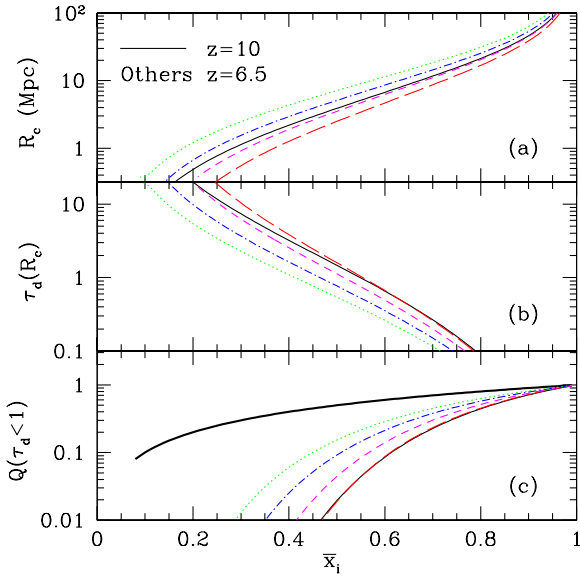


**Figure 1.** (a): The characteristic bubble size  $R_c$  throughout reionization. (b): The damping wing optical depth  $\tau_d$  at the center of a bubble of the size  $R_c$ . (c): The fraction of the universe filled by bubbles with  $\tau_d < 1$  (as measured from the center of each bubble). In each panel, the solid and long-dashed curves take  $m_{\min} = m_4$  at  $z = 10$  and  $z = 6.5$ , respectively. The short-dashed, dot-dashed, and dotted curves take  $z = 6.5$  and  $m_{\min}/m_4 = 3, 10$ , and  $30$ , respectively. The thick solid line in the bottom panel shows  $Q = \bar{x}_i$ .

where  $\delta_c$  is the critical density for spherical collapse.

The FZH04 model includes recombinations in only a crude sense (as a global average number of recombinations per baryon). Furlanetto & Oh (2005) showed how to incorporate them in a more physically plausible manner. For a bubble to grow, the (local) mean free path of an ionizing photon must exceed its radius. The mean free path is determined by the spatial extent and number density of dense, neutral blobs (where the recombination time is short). Thus, as a bubble grows, its internal radiation background must also increase to ionize each of these blobs more deeply. As a consequence, the recombination rate inside the bubble also increases; HII regions saturate when this recombination rate exceeds the ionizing emissivity (see also Miralda-Escudé et al. 2000). Furlanetto & Oh (2005) showed that, for reasonable models of the IGM density field, recombinations halt the evolution at a well-defined radius  $R_{\max}$ ; any bubbles nominally larger than this size fragment into regions with  $R \approx R_{\max}$ . (Note, however, that this saturation radius describes the mean free path of ionizing photons, not the extent of contiguous ionized gas; obviously as  $\bar{x}_i \rightarrow 1$  ionized gas does fill the universe.) Unfortunately, calculating  $R_{\max}$  requires knowledge of the IGM density field during reionization, which we currently lack. We will therefore leave it as a free parameter, noting that  $R_{\max} \gtrsim 20$  Mpc if the density field is similar to that at  $z \sim 2-4$  (Miralda-Escudé et al. 2000), but minihaloes could in principle reduce it to  $R_{\max} \lesssim 5$  Mpc.

### 3 THE EVOLVING LUMINOSITY FUNCTION

We will now examine how the FZH04  $n_b(m)$  affects the visibility of Ly $\alpha$ -selected galaxies throughout reionization. A full model

requires two elements: a prescription for associating Ly $\alpha$  line luminosity with halo mass and a prescription for the damping wing absorption  $\tau_d$ . The latter is straightforward: to a first approximation, it depends only on the distance from the galaxy to the edge of its HII region, which determines the amount by which each photon redshifts away from line center before encountering the neutral gas, and the mean ionized fraction of the absorbing gas. The velocity dispersions of high-redshift galaxies are  $\approx 12(m/m_4)^{1/3} \text{ km s}^{-1}$ , while the velocity width of a bubble is  $\sim 100(R/\text{Mpc}) \text{ km s}^{-1}$ . Thus the damping wing absorption is nearly constant across the line throughout most of reionization (for a specific example, see Fig. 5 of Furlanetto et al. 2004a). We use the formula of Miralda-Escudé (1998) assuming that gas with  $\bar{x}_i$  extends along a path length  $\Delta z = 0.5$  from the edge of the HII region. This choice is somewhat arbitrary, but our results are not sensitive to it:  $\tau_d$  changes by  $\lesssim 5\%$  so long as  $\Delta z > 0.25$  and only  $\sim 20\%$  for  $\Delta z = 0.1$ . Thus, unless the mean ionized fraction evolves extremely rapidly, it should be a reasonable estimate. On the other hand, because the damping wing integrates over a large path length (effectively  $\gtrsim 50$  comoving Mpc) it is relatively insensitive to fluctuations in the ionized fraction outside of the host bubble. For simplicity, we set  $\tau_d$  equal to its value at the center of each bubble.

Note that we ignore a number of potential complications here. The most obvious is resonant absorption by residual neutral gas within each bubble. FHZ04 (among many others) have included this effect; for typical galaxies, the resonant absorption has  $\tau_\alpha \gtrsim 1$  blueward of the line center, which eliminates the flux on the blue side of the line. However, with this optical depth the absorption from each volume element is quite narrow in redshift space (i.e. the associated damping wings are negligible), so the effective optical depth for photons that begin on the red side of the line is much smaller than unity (see Fig. 5 of FHZ04 for an illustrative example). Thus, to first order, resonant absorption eliminates about half of the flux from each galaxy; we can incorporate this into our model by simply reducing the assumed intrinsic luminosity of each galaxy by a factor of two. This approximation ignores the fact that the ionizing radiation field is stronger around brighter galaxies, reducing the effective resonant optical depth; this would imprint a trend with galaxy mass that our model does not include. However, a number of other effects could mitigate this trend. Most importantly, the properties of individual galaxies, such as infall regions and winds, move the relative velocities of the line and the absorbing gas (Santos 2004). If winds, for example, move the emission to the red side of the line – as occurs in lower-redshift samples (e.g., Shapley et al. 2003) – resonant absorption becomes completely unimportant. Moreover, with our large bubbles the average ionizing background can make a non-negligible contribution. The galaxy’s neighbours might also matter, because galaxies are clustered even inside the bubbles. All of these effects would tend to decrease the difference in resonant absorption between bright and faint galaxies; thus we have chosen to ignore this aspect in our model. We also neglect the spatial distribution of galaxies within each bubble and the clustering of bubbles (see §4).

Computing the Ly $\alpha$  line luminosity of each galaxy is much more problematic. There is no simple analytic model for this quantity, although Le Delliou et al. (2005a) have shown that semi-analytic models can match the observed luminosity functions over a range of redshifts by assuming a flat, top-heavy initial mass function and a constant escape fraction of ionizing photons (see also Le Delliou et al. 2005b). There are two obvious hurdles: the Ly $\alpha$  luminosity should vary in time with the star formation rate and vary spatially with the distribution of dust and other absorb-

ing gas within the galaxy (particularly winds). Simulations include the former effect (at least in principle), but at lower redshifts the number density of star-forming galaxies in simulations (which already include the time variability) exceeds the number density of observed Ly $\alpha$ -emitters by about an order of magnitude (Furlanetto et al. 2005b) even though the same simulations match the history of cosmic star formation (Springel & Hernquist 2003; Hernquist & Springel 2003, but see Nagamine et al. 2004b) and the observed Lyman-break population (Nagamine et al. 2004a; Night et al. 2005) reasonably well. The remaining discrepancy can reasonably be attributed to geometry; for example, Shapley et al. (2003) find that only  $\sim 20\%$  of Lyman-break galaxies at  $z = 3$  have Ly $\alpha$  emission lines, with a hint that lower-luminosity galaxies tend to have stronger lines. How these factors evolve with redshift is not well-constrained. Shapley et al. (2003) find that younger galaxies are less likely to have Ly $\alpha$  emission lines. On the other hand, direct comparison of the number counts of continuum-selected and Ly $\alpha$  line-selected galaxies suggests that the fraction of galaxies with strong Ly $\alpha$  lines may increase with redshift. In the absence of better constraints, we will assume that the Ly $\alpha$  luminosity of each galaxy is  $L_\alpha \propto \zeta m_h \propto m_h$  so that – if there were no IGM absorption – a particular survey could detect every galaxy with  $m_h > m_{\text{obs,min}}$ . While clearly simplistic, this serves to illustrate our point. So long as the geometric effects eliminate a random fraction of the population, they will not affect our conclusions. More worrying is the assumption that  $\zeta = \text{constant}$ . We find, however, that this does not qualitatively affect the argument, although it does modify the resulting numerical constraints (see §5).

Figure 1 illustrates the major effects we expect from the evolving bubble population. The characteristic bubble size grows rapidly with  $\bar{x}_i$ , decreasing the mean absorption suffered by a typical galaxy (see Figure 1b). Thus the Ly $\alpha$  galaxy abundance should begin to fall significantly once  $\bar{x}_i \sim 0.5$ , beyond which  $\tau_d(R_c) \gtrsim 1$ . However, even if  $R_c$  is small, some larger bubbles still exist. Figure 1c shows the fraction of space  $Q$  filled by bubbles with  $\tau_d < 1$ . These large bubbles are crucial for observing sources at early times. On the other hand,  $Q \rightarrow \bar{x}_i$  near the end of reionization because  $R_c$  moves well beyond the required scale.

More precisely, equation (2) allows us to compute the distribution of galaxies within each bubble and hence the distribution of  $\tau_d$  (FHZ04 give a closely related calculation). With the assumption that  $L_\alpha \propto m_h$ , a galaxy of mass  $m_h$  will lie in the survey if

$$\tau_d < \ln \left( \frac{m_h}{m_{\text{obs,min}}} \right). \quad (3)$$

Given a bubble of mass  $m_b$ , equation (3) implicitly yields the minimum mass  $m_{h,\text{min}}$  for a member galaxy to lie in our survey. Thus the total number density of observable galaxies is

$$n(>L) = \int dm_b n_b(m_b) V_b \int_{m_{h,\text{min}}}^{m_b/\zeta} dm_h n_h(m_h|m_b), \quad (4)$$

where  $V_b$  is the bubble volume.

We show some examples of the resulting luminosity functions at  $z = 6.5$  in Figure 2. The thick solid line in panel (a) is the assumed intrinsic luminosity function (neglecting absorption, appropriate if  $\bar{x}_i = 1$ ). The long-dashed, short-dashed, and dotted curves assume  $\bar{x}_i = 0.75, 0.5$ , and  $0.25$ , respectively. Panel (b) shows the ratio of  $n(>L)$  after attenuation to its value in a universe with  $\bar{x}_i = 1$ .

We find that  $n(>L)$  remains substantial even in the mid-stages of reionization: galaxies do not begin to disappear in

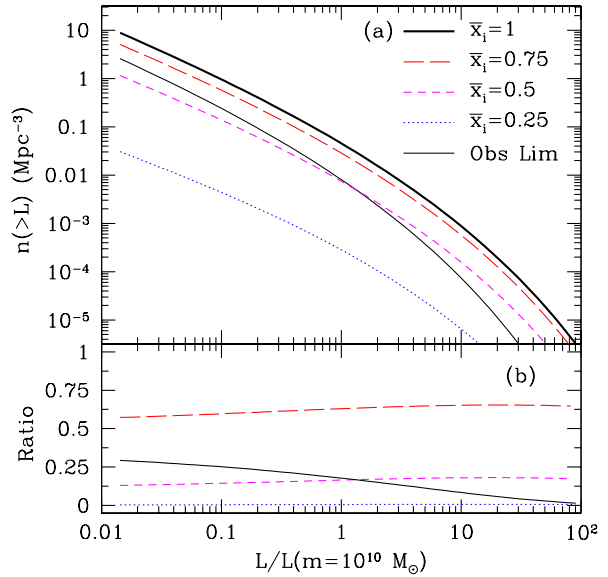


**Figure 2.** (a): Ly $\alpha$  luminosity functions at  $z = 6.5$ . The thick solid line shows the assumed intrinsic function (with  $L_\alpha \propto m_h$ ). The thin solid line shows the observational limit of Malhotra & Rhoads (2004), corresponding to attenuation by a factor of three in comparison to the  $z = 5.7$  luminosity function. The other curves show how  $n(>L)$  is affected by the bubble size distribution. (b): Ratio of the attenuated to intrinsic luminosity functions.

large numbers until  $\bar{x}_i \lesssim 0.5$ . We find the relative magnitude of the decline to be nearly independent of redshift, because  $n_b(m)$  at a given  $\bar{x}_i$  is also largely independent of redshift (and the mean optical depth compensates for most of the remaining evolution; see Fig. 1b). The number counts decline by  $\sim 2$  when  $\bar{x}_i = 0.75$  and  $\sim 10$  when  $\bar{x}_i = 0.5$  so long as  $L_\alpha \propto m_h$ . Interestingly, we find that – at least in this simple model – the ratio of the attenuated and intrinsic luminosity functions is nearly independent of galaxy luminosity. This is a result of two competing effects. First, larger galaxies tend to reside in larger bubbles (although this trend is much weaker than if galaxies were isolated), suffering correspondingly weaker absorption. However, the mass function steepens toward higher masses: thus if all galaxies suffered identical absorption (as in the thin solid curves; see below), the ratio would decrease sharply at large  $L$  because a fixed luminosity interval causes a much larger decrease in the number counts. Evidently these two effects nearly compensate. If this remains true in more sophisticated models, it would be useful in that it removes the degeneracy of Ly $\alpha$  galaxy tests of reionization with the intrinsic luminosity limit of a survey. Note that, if resonant absorption is stronger around faint galaxies, it would flatten the luminosity function and make bright galaxies somewhat easier to see than faint galaxies (see the second paragraph of this section).

Malhotra & Rhoads (2004) compared the  $z = 5.7$  and  $z = 6.5$  luminosity functions of Ly $\alpha$ -selected galaxies and found no evidence for evolution; formally they ruled out a model in which each galaxy’s line is attenuated by a factor of three. We show their constraint (translated to our assumed luminosity function) by the thin solid line. To place a quantitative constraint, we must associate their luminosity threshold with a halo mass. The number density of detected  $z = 6.5$  galaxies in their sample is  $n \sim 10^{-4} \text{ Mpc}^{-3}$ , which would correspond to  $m \sim 10^{11.5} \text{ M}_\odot$  if there were a one-to-one correspondence between haloes and Ly $\alpha$ -emitters. Such a large

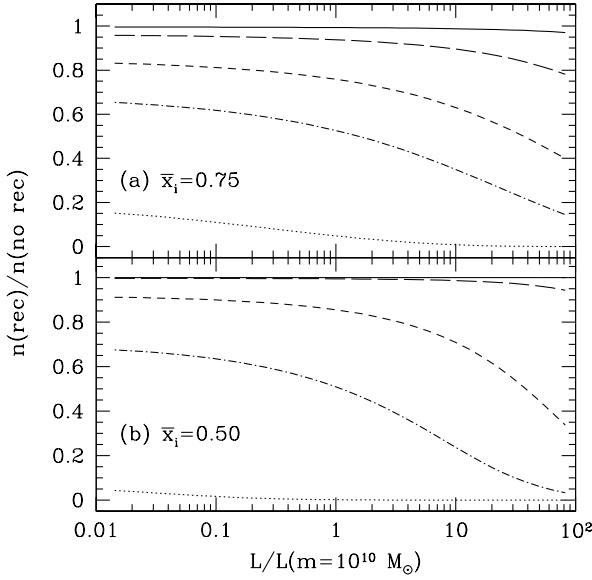


**Figure 3.** Number density of galaxies above a luminosity  $L$  at  $z = 6.5$  if recombinations impose a maximum bubble size  $R_{\max}$ , relative to their abundance without an imposed maximum size. In each panel, the solid, long-dashed, short-dashed, dot-dashed, and dotted curves take  $R_{\max} = 20, 10, 5, 3$ , and  $1$  Mpc, respectively.

mass implies a weak constraint,  $\bar{x}_i \gtrsim 0.35$ . However, comparison to simulations at lower redshifts indicates that fewer than  $\sim 10\%$  of haloes actually host Ly $\alpha$  lines (Furlanetto et al. 2005b). This would place the limit at  $\bar{x}_i \gtrsim 0.5$ . A more precise constraint must await a more satisfactory model of Ly $\alpha$ -emitters, including their detailed intrinsic properties (such as winds, which can move the Ly $\alpha$  line in velocity space and allow more transmission than otherwise expected). However, we note that our model should be relatively robust to these details, because the length scales of our bubbles are many times larger than those considered by, e.g., Santos (2004).

Obviously, transmission relies on the existence of large HII regions. By imposing a maximum effective bubble size  $R_{\max}$ , recombinations eliminate the largest bubbles (Furlanetto & Oh 2005). We can approximately incorporate this by assuming that the damping wing absorption begins at  $R_{\max}$  for any galaxy nominally in a bubble larger than this radius (Fig. 9 of Furlanetto & Oh 2005 shows this to be a reasonable approximation). Figure 3 illustrates the effect on the luminosity function. We show the fraction of galaxies above a given luminosity threshold that are visible relative to the case with  $R_{\max} = \infty$ . We show a range of values for  $R_{\max}$ , which is quite uncertain because of our poor knowledge of the density structure of the IGM during reionization.

A number of trends are apparent in Figure 3. First, recombinations only significantly affect  $n(> L)$  if  $R_{\max} \lesssim 5$  Mpc;  $\tau_d$  is sufficiently small in larger bubbles that restricting their sizes makes little difference. Thus the luminosity function will be unaffected if the density model of Miralda-Escudé et al. (2000) – which essentially extrapolates the population of Lyman-limit systems at  $z \sim 3$  – is accurate. Second,  $R_{\max}$  affects brighter galaxies more strongly, because their mass function is steeper and they reside in larger bubbles. Third,  $n(> L)$  is more sensitive to  $R_{\max}$  at  $\bar{x}_i = 0.75$  because more of the universe is contained in bubbles with nominal  $R > R_{\max}$ . That trend reverses itself if  $R_{\max} \ll R_c$ , in which case the mean neutral fraction in the absorbing gas dom-

inates the effect (as in the dotted curves). (Note that this simple treatment may overestimate the effect of imposing an  $R_{\max}$ : small recombination-limited bubbles cluster strongly, rendering the absorption somewhat weaker than our simple  $\tau_d$  calculation would predict.)

#### 4 THE OBSERVED CORRELATION FUNCTION

FHZ04 pointed out that, in addition to decreasing the mean number density of observable galaxies, the HII regions will modify their spatial distribution. Here we show how this affects their clustering. Dwarf galaxies could appear in a survey at  $\bar{x}_i \ll 1$ , but they will be confined to the small volume filled by (rare) large bubbles. On the other hand, each of these bubbles contains many galaxies. A simple model illustrates how this enhances the apparent clustering on small scales (relative to galaxies observed in the continuum, for example). Suppose that galaxies with number density  $\bar{n}$  are distributed randomly throughout the universe but that we can only observe those with at least one neighbour within a sphere of volume  $V \ll \bar{n}^{-1}$ . Assuming a Poisson distribution, the number density of observed objects would be  $n_{\text{obs}} = \bar{n}(1 - e^{-\bar{n}V})$ . As usual the correlation function of the observed sample is defined through the total probability of finding two galaxies in volumes  $\delta V_1$  and  $\delta V_2$ ,  $\delta P = n_{\text{obs}}^2 (1 + \xi) \delta V_1 \delta V_2$ . However, we know that every observed galaxy has a neighbour within  $V$ ; thus  $\delta P = n_{\text{obs}} \delta V_1 (\delta V_2/V)$  for small separations (where the factor  $\delta V_2/V$  assumes the neighbour to be randomly located within  $V$ ). Thus,  $\xi = 1/(n_{\text{obs}}V) - 1$  on such scales: even though the underlying distribution is random, the selection criterion induces clustering. Note that it can be extremely large if  $V \ll n_{\text{obs}}^{-1}$ .

On large scales, the modulation takes a different form. An observed galaxy resides in a large bubble, corresponding to an overdense region. Because such regions are biased (i.e. more strongly clustered than the underlying mass distribution), they will tend to lie near to other overdense regions – and hence to other large bubbles. Thus, we will be more likely to see galaxies near the original object than in an average slice of the universe. Because we do not see similar galaxies in small (less-biased) bubbles, the large-scale bias will generically be larger than that intrinsic to the galaxies.

Because these two effects have different amplitudes, the bubbles introduce a scale-dependent bias to the correlation function of galaxies, with a break at  $r \approx R_c$ . Unfortunately, developing a self-consistent analytic model for the correlation function  $\xi(r)$  is difficult because spherical bubbles introduce spurious features on scales  $\sim R_c$ , just the regime in which the scale dependence is most interesting. These features occur because of the difficulty of efficiently filling space with non-overlapping spheres (see the discussion in McQuinn et al. 2005). Instead we will compute the limiting cases of  $r \ll R_c$  and  $r \gg R_c$ .

By analogy with the halo model for the density field (Cooray & Sheth 2002), these limiting regimes correspond to correlations between galaxies within a single bubble and within two separate bubbles. We begin with large scales: the observed clustering is the average bias of the bubbles weighted by the number of galaxies in each HII region (analogous to the two-halo term for the density field):

$$b_{r=\infty} = \int dm_b n_b(m_b) b_b(m_b) V_b \times \int_{m_{h,\min}}^{m_b/\zeta} dm_h \frac{n_h(m_h|m_b)}{\bar{n}_{\text{gal}}}, \quad (5)$$

where we integrate only over those haloes visible after damping wing absorption and  $\bar{n}_{\text{gal}}$  is the mean number density of observable galaxies. Following the procedure of Mo & White (1996), the bias  $b_b$  of HII regions is (McQuinn et al. 2005)

$$b_b(m_b) = 1 + \frac{B(m_b)/\sigma^2(m_b) - 1/B_0}{D(z)}, \quad (6)$$

where  $D(z)$  is the linear growth factor. Here and throughout we work with the linear bias  $b$ , which is defined by  $n(m|\delta) = n(m)[1 + b\delta + \mathcal{O}(\delta^2)]$  for a population with mean number density  $n(m)$ . Note that (unlike the halo bias) we can have  $b_b < 0$ : late in reionization, small bubbles are truly *anti*-biased because dense regions have already been incorporated into large ionized regions. Unfortunately, as discussed by McQuinn et al. (2005), our linear bias formula breaks down late in reionization, essentially because the physical requirement that  $x_i \leq 1$  caps the effective number density and hence the bias. By comparing to the FZH04 ionization model as implemented in numerical realisations of gaussian random fields, McQuinn et al. (2005) found that equation (6) overpredicts the biasing when  $\bar{x}_i \sim 1$ . Our quantitative predictions for large  $\bar{x}_i$  should therefore be taken with caution.

The behaviour on small scales is somewhat more subtle. If galaxies were randomly distributed within each bubble, the simple argument in the first paragraph of this section suggests that the correlation function would just be the weighted average of the number of pairs per HII region. However, in addition to the increase in the number of galaxies in each bubble, the galaxies also trace density fluctuations within each bubble. We therefore write

$$b_{\text{sm}}^2 = \int dm_b n_b(m_b) V_b b_h^2(m_b) \frac{\langle N_{\text{gal}}(N_{\text{gal}} - 1)|m_b \rangle}{\bar{N}_{\text{gal}}^2}, \quad (7)$$

where  $\bar{N}_{\text{gal}} = \bar{n}_{\text{gal}} V_b$ ,  $\langle N_{\text{gal}}(N_{\text{gal}} - 1)|m_b \rangle$  is the expected number of galaxy pairs within each bubble, and  $b_h^2$  measures the excess bias of these haloes inside each bubble.<sup>1</sup> We note that equation (7) ignores nonlinear corrections to the density field (the one-halo term), which dominate on scales of tens of kpc at these redshifts. It therefore applies only to separations intermediate between this nonlinear scale and  $R_c$ .

We can write the expected number of pairs as

$$\begin{aligned} \langle N_{\text{gal}}(N_{\text{gal}} - 1)|m_b \rangle &\approx V_b \int dm_h n_h(m_h|m_b) (V_b - \zeta m_h/\bar{\rho}) \\ &\times \int^{m_{\text{max}}} dm'_h n_h(m'_h|m_b), \end{aligned} \quad (8)$$

where the factor in parentheses accounts for the “bubble exclusion effect”: the total mass of galaxies within a specified bubble cannot exceed  $m_b/\zeta$  or we would overproduce the number of ionizing photons. This also sets  $m_{\text{max}} = m_b - \zeta m_h$ . Because most galaxies have  $m_h \sim m_{\text{min}} \ll m_b/\zeta$ , we will take  $m_{\text{max}} = m_b/\zeta$  but begin the integration over  $m_b$  in equation (7) at  $2\zeta m_{\text{min}}$  in order to exclude bubbles that can contain only a single galaxy. With these simplifications,

<sup>1</sup> This expression can be derived formally (modulo the precise definition of  $b_h^2$ ; see below) by constructing the galaxy density field from bubbles and their constituent haloes, in analogy to the halo model. It corresponds to the “two-halo, one-bubble” term in such a treatment; i.e., correlations between two particles that lie in the same bubble but different dark matter haloes. The “bubble profile” describing the distribution of galaxies within the bubble turns out to be proportional to the square root of the linear matter correlation function.

$$\langle N_{\text{gal}}(N_{\text{gal}} - 1)|m_b \rangle \approx \max\{0, \bar{N}_{\text{gal}}(m_b)[\bar{N}_{\text{gal}}(m_b) - 1]\}. \quad (9)$$

This approximation is reasonable so long as most of the observed galaxies are in bubbles with  $\bar{N}_{\text{gal}} \gtrsim 2$ ; if this is not true, then we would underestimate the clustering because the pair count is dominated by small bubbles with an unusual galaxy distribution. This only happens if the luminosity threshold in the survey is extremely large or at quite high redshifts (for example, a survey at  $z = 15$  with  $m_{\text{obs,min}} = 10^{10} M_{\odot}$  encounters these problems). In particular, our approximation is valid for all the cases we show here. Of course, the first high-redshift surveys may only see the brightest galaxies and so lie within the regime where our formalism breaks down. Properly interpreting small-scale clustering in such cases requires more sophisticated methods, in particular numerical simulations or hybrid approaches similar to Zahn et al. (2005).

The remaining factor is  $b_h(m_b)$ . It may seem reasonable to take this to be the mean value of the usual Mo & White (1996) halo bias, evaluated over  $n_h(m_h|m_b)$ . However, the pair density inside each bubble *already* includes much of this bias because it counts the number of galaxies in a region with overdensity  $\delta_x$ . We therefore only want the “excess” bias of the galaxies relative to density fluctuations on scales smaller than  $m_b$ , which is the bias evaluated from the conditional mass function in equation (2). Following the procedure of Mo & White (1996), we find

$$b_h(m_h|m_b) = 1 + \frac{(\delta_c - \delta_x)^2/(\sigma^2 - \sigma_b^2) - 1}{\delta_c(z=0) - \delta_x(z=0)}. \quad (10)$$

Because the presence of the first galaxy in a pair biases the second to be smaller than average (the bubble exclusion effect mentioned above), we take

$$b_h^2(m_b) \approx \langle b_h|m_b \rangle b_h(m_{h,\text{min}}), \quad (11)$$

where  $\langle b_h|m_b \rangle$  is the average of equation (10) over  $n_h(m_h|m_b)$ . This will slightly underestimate the true bias by forcing all of the galaxy’s neighbours to be of the minimum possible size (and hence bias).

We show the resulting bias at  $z = 10$  (as a function of  $\bar{x}_i$ ) in Figure 4. In each panel, the solid, long-dashed, and short-dashed curves take  $m_{\text{obs,min}} = m_4$ ,  $10^9 M_{\odot}$ , and  $10^{10} M_{\odot}$ , respectively. Panels (a) and (b) show  $b_{\text{sm}}$  and  $b_{r=\infty}$ . We scale the results to the bias  $\bar{b}_h$  intrinsic to the galaxy population if absorption could be ignored. Panel (c) shows the ratio  $b_{r=\infty}/b_{\text{sm}}$ , illustrating the magnitude of the “break” in the linear bias. We emphasize that the scale at which the break occurs will evolve throughout reionization along with the characteristic bubble size  $R_c$ ; for illustrative purposes we mark several values of  $R_c$ .

Before commenting on our results, we note that the approximations in the FZH04 model, equation (6), and the treatment of galaxy pairs will obviously cause errors in the predicted bias. Fortunately, we can check these by noting that we should recover  $\bar{b}_h = b_{\text{sm}} = b_{r=\infty}$  if we neglect absorption entirely by including *all* galaxies in each bubble. Here  $\bar{b}_h = \int dm n_h(m) b_h(m) / \int dm n_h(m)$  is the actual mean bias of the galaxy population. The dotted curves in panels (a) and (b) compare the recovered values to the true bias. Without absorption, equation (5) is equivalent to an integral over the halo mass function; the bubble bias is essentially the same as the average bias of the haloes it contains, so the resulting errors are typically  $\lesssim 10\%$  (and furthermore do not vary much with  $\bar{x}_i$ ). The small-scale result in equation (7) becomes the weighted average of the bias of pairs of galaxies in each bubble, where the galaxy bias is built from the conditional  $b_h(m_h|m_b)$  and the number of pairs. Panel (a) shows that

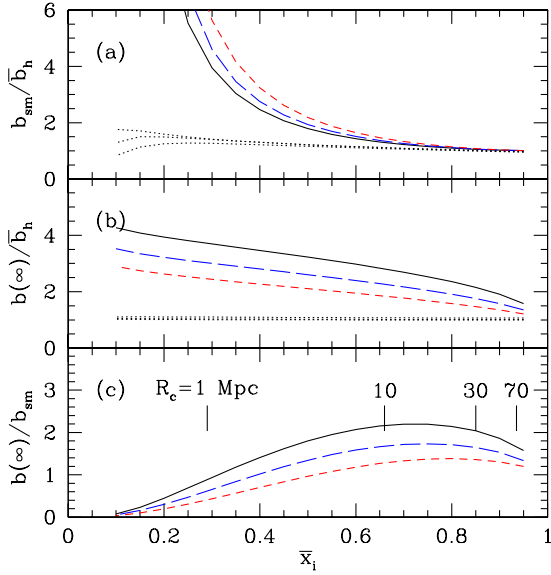


**Figure 4.** (a): Predicted small-scale bias at  $z = 10$ , relative to the bias expected if all galaxies above the mass threshold were visible. This applies to separations larger than the nonlinear scale but smaller than  $R_c$ . The solid, long-dashed, and short-dashed curves take  $m_{\text{obs,min}} = m_4, 10^9$ , and  $10^{10} M_\odot$ , respectively. The dotted curves show the predicted *absorption-free* galaxy bias relative to its true value (see text). (b): Predicted large-scale bias at  $z = 10$ , relative to the bias expected if all galaxies above the mass threshold were visible. (c): Ratio of large to small scale bias. We mark the characteristic bubble size  $R_c$  (in Mpc) as well.

the formalism is accurate for moderate to large  $\bar{x}_i$  but encounters problems when  $\bar{x}_i$  is small. At worst this error is a factor  $\sim 2$ . We are primarily interested in the observable bias relative to the intrinsic value, so we attempt to remove this error by scaling all of our curves in units of the predicted value, rather than the true intrinsic bias. Note, however, that it makes a significant difference only for  $\bar{x}_i$  near the minimum value shown in each plot.

Clearly, both  $b_{\text{sm}}$  and  $b_{r=\infty}$  decrease throughout reionization. The large-scale bias decreases because the ionized regions must lie nearer to the mean density (and hence be less biased) as  $\bar{x}_i \rightarrow 1$ : this behaviour must be generic to any model in which reionization begins in overdense regions. The small-scale bias decreases because bubbles large enough to allow transmission become common: early on, only those galaxies with near neighbours are visible, so the correlations are strong. In the middle and final stages of reionization, most galaxies lie inside bubbles large enough to permit transmission, so more typical galaxies become visible and  $b_{\text{sm}} \rightarrow \bar{b}_h$ .

Note that  $b_{r=\infty}/\bar{b}_h$  decreases with  $m_{\text{obs,min}}$  in panel (b). This may seem counterintuitive, because more massive galaxies are also more highly biased. In fact it is true that the value of  $b_{r=\infty}$  increases with  $m_{\text{obs,min}}$ , but the amplification relative to the underlying population is larger for small galaxies. Large galaxies preferentially sit in large bubbles and so suffer relatively little absorption. But a large fraction of small galaxies reside in small bubbles, where they disappear because of damping wing absorption. Thus the Ly $\alpha$  selection picks out a more unusual population of small galaxies than it does for large galaxies, explaining the former's increased amplification. If the resonant absorption decreases with halo mass (see the discussion in §3), that would exaggerate this trend, because

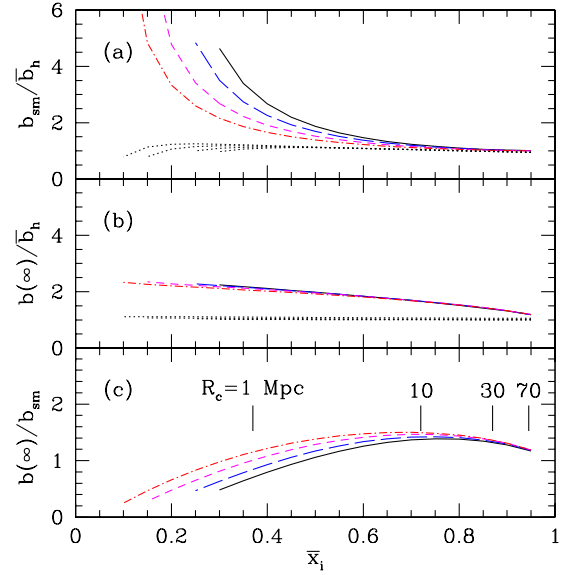


**Figure 5.** As Fig. 4, but for  $z = 6.5$ . All the curves take  $m_{\text{obs,min}} = 10^{10} M_\odot$ . The solid, long-dashed, short-dashed, and dash-dotted curves take  $m_{\text{min}}/m_4 = 1, 3, 10$ , and  $30$ , respectively. We mark  $R_c$  for  $m_{\text{min}} = m_4$  here; see Fig. 1a for  $R_c$  in the other scenarios.

faint galaxies would have to sit in even larger bubbles. (For the same reason, it would also increase the small-scale bias.)

As emphasized above, the transition between these two regimes occurs on scales  $r \approx R_c$ . Measuring the location of the break will thus directly constrain  $n_b(m)$ . Interestingly, our model also shows significant evolution in  $b_{r=\infty}/b_{\text{sm}}$  throughout reionization, offering an independent measure of  $\bar{x}_i$ . Early in reionization, the small-scale bias dominates because large bubbles are extremely rare (a survey would find a few distinct clumps of galaxies, even though the underlying galaxy distribution is fairly uniform; the clustering on scales smaller than the average clump thus appears enormous). However, once a typical bubble grows enough to allow significant transmission, the small-scale bias rapidly falls to that intrinsic to the haloes (compare to Figure 1b). Meanwhile, the large-scale bias remains substantial (subject to the caveat that our linear treatment eventually breaks down) – these bubbles are overdensities on scales much larger than the typical galaxy, so they cluster more strongly. Thus toward the end of reionization  $b_{r=\infty}$  is typically larger by a factor of order unity; the ratio increases slowly as  $z$  increases.

Figure 5 shows the bias for a survey with  $m_{\text{obs,min}} = 10^{10} M_\odot$  at  $z = 6.5$ . Here, we vary the minimum halo mass to host a galaxy,  $m_{\text{min}}$ . Comparing the solid curves in Figures 4 and 5, we find that the induced large-scale bias decreases with cosmic time, but the small-scale bias does not change dramatically. Interestingly, the mass threshold has virtually no effect on the large-scale bias: although  $n_b(m)$  shifts to larger scales, the bias averaged over each distribution remains nearly constant. However, by increasing  $R_c$ , the modulation becomes less severe and  $b_{\text{sm}}$  decreases at a fixed  $\bar{x}_i$ . Thus the small-scale bias early in reionization is also sensitive to the bubble size distribution.

## 5 DISCUSSION

We have shown that the sizes of HII regions during reionization strongly affect the distribution of Ly $\alpha$ -selected galaxies (see also FHZ04). The neutral IGM extinguishes the Ly $\alpha$  lines of galaxies, reducing their number counts. Without source clustering, their abundance declines significantly when  $\bar{x}_i \lesssim 0.7$ – $0.9$ , with the range depending on assumptions about the detailed intrinsic properties of the galaxies (Santos 2004). In our model, the existence of large HII regions implies that their abundance only begins to decline when  $\bar{x}_i \lesssim 0.5$ . This weakens existing constraints on the neutral fraction at  $z = 6.5$  (Malhotra & Rhoads 2004), but it also implies that the Ly $\alpha$  selection technique will be useful even into the middle stages of reionization.

Moreover, we have shown that the extinction is not uniform across the sky – galaxies in large HII regions remain visible, but those in smaller bubbles vanish. The bubbles thus induce extra clustering in the galaxy distribution. On large scales, the observed galaxies trace the highly-biased large bubbles. On small scales, the clustering increases rapidly at early times because only those exceptional regions with an excess of galaxies are visible. As a result, we expect a break in the observed bias to appear on the typical scale of the HII regions, with a magnitude that evolves throughout reionization. Thus large area surveys for Ly $\alpha$ -emitters have the potential to offer powerful constraints on the topology of neutral gas during reionization.

One potential obstacle to interpreting the luminosity function and clustering measurements is our poor knowledge of the intrinsic properties of these galaxies. The luminosity function test is clearest as a differential measurement between two nearby redshifts (as indeed Malhotra & Rhoads 2004 applied it), because that decreases the amount of evolution one would expect in the intrinsic source population. However, if reionization is extended, such differential tests may not offer much insight. Clustering can encounter similar difficulties: lower redshift Ly $\alpha$  galaxies are highly clustered (Hamana et al. 2004; Ouchi et al. 2005), and it may seem difficult to extract information about reionization without understanding their intrinsic properties. In particular, the density of Ly $\alpha$ -selected galaxies at  $z = 5.7$  shows rather large variations on large scales (Ouchi et al. 2005). More effort is clearly needed to understand these systems, and their lower-redshift analogues, in greater depth.

Fortunately, there is one strategy that may allow us to sidestep these difficulties: we can compare Ly $\alpha$ -selected samples to samples collected through other techniques, such as broadband Lyman-break selection. Provided that the latter can be corrected for the effects of the Ly $\alpha$  line properties on continuum selection (which may not be trivial) and that the average line properties of galaxies of a given luminosity do not evolve rapidly with redshift, they can be used as a control sample. For example, if the number counts of Ly $\alpha$ -selected galaxies decline several times faster than Lyman-break galaxies over some redshift interval, that would constitute strong evidence for a significant change in  $\bar{x}_i$ . The Lyman-break sample can also be used to estimate the evolution of the intrinsic halo bias as a control for measurements of the small and large-scale bias induced by the bubbles. (Note that the clustering also offers another consistency check: the intrinsic galaxy bias should be independent of separation, but Ly $\alpha$  absorption induces a scale-dependent feature that evolves throughout reionization.) Thus, the Ly $\alpha$  and Lyman-break selection techniques nicely complement each other. There are three caveats to this approach, however. First, the Ly $\alpha$  line may have a non-trivial effect on the photometric selec-

tion. Second, there is some weak evidence that Ly $\alpha$  line properties do evolve at lower redshifts, although this would only be a problem if the evolution occurs on a shorter timescale than changes in  $\bar{x}_i$ . Finally, continuum-selection techniques often have difficulty reaching similar depths to line-selection, which will restrict the available range of line luminosities.

Our models are extremely simple, and one can imagine any number of complications. However, our qualitative conclusions are robust. For example, we have assumed the ionizing efficiency of galaxies to be independent of their mass. Furlanetto et al. (2005a) show how to relax this assumption within the context of the FZH04 model. They find that making  $\zeta$  an increasing function of halo mass will increase  $R_c$  because it boosts the average bias of the underlying galaxy population. Thus the damping wing absorption decreases at a given  $\bar{x}_i$ , allowing Ly $\alpha$  selection to penetrate even deeper into the reionization epoch. For instance, if  $\zeta \propto m^{1/3}$  at  $z = 6.5$ , half the galaxies disappear when  $\bar{x}_i \sim 0.5$  (compared to half at  $\bar{x}_i \sim 0.75$  if  $\zeta = \text{constant}$ ; see Fig. 2). Such an assumption also tends to reduce the boost in small-scale bias at early times, but it does not affect the existence of the break in clustering at  $\sim R_c$ .

We also showed that incorporating recombinations can significantly reduce the number counts of Ly $\alpha$ -selected galaxies by imposing a maximum size on the bubbles, but only if the IGM is much clumpier than an extrapolation from  $z \sim 3$  would imply (Miralda-Escudé et al. 2000). Such clumpiness may not be surprising, because Jeans smoothing is much less effective if the gas remains cold until photoionization (e.g., Iliev et al. 2005). It will also affect the clustering: in such a picture large bubbles require a substantial excess of sources, boosting the small-scale bias by an even larger amount than in the FZH04 model. Furthermore, it affects the characteristic size of the HII regions and so changes the location of the expected break in the clustering strength.

Our analytic models are only approximate, and our predictions can be improved with numerical techniques, even short of full cosmological simulations. For example, applying the FZH04 ionization criterion to numerical simulations or gaussian random fields (as in Zahn et al. 2005) will allow us to include the distribution of galaxies within each bubble, the (non-spherical) morphology of bubbles, their proper biasing for large  $\bar{x}_i$ , and analyze galaxy samples restricted to the brightest objects. Such an approach will yield predictions for the full, scale-dependent correlation function of Ly $\alpha$ -selected galaxies, which will allow much more detailed comparisons with future observations. Complete numerical simulations with radiative transfer will allow even more sophisticated tests of the model, including our treatment of recombinations, source clustering, and the intrinsic clumpiness of the IGM.

Our results have a number of implications for ongoing and future searches for high-redshift Ly $\alpha$ -emitters. First and foremost, our robust prediction of large HII regions implies that this selection technique will allow us to probe farther back in the reionization process than one might have naively expected. Thus, it is crucial to push these surveys to the highest redshifts possible. Once galaxies are detected at a particular redshift, we advocate extending the search to as wide a contiguous area as possible in order to measure the clustering. Even though constructing a catalogue sufficiently deep to measure the large-scale bias may be impractical given telescope time constraints, any detection of extremely large small-scale clustering would offer strong evidence for a relatively large neutral fraction. Studies like these, combined with other probes of the high redshift IGM such as 21 cm emission (e.g. Zaldarriaga et al. 2004), therefore have the potential to reveal how reionization de-

veloped and to elucidate the sources responsible for this process (e.g. Furlanetto et al. 2004c).

We thank an anonymous referee for helpful comments that improved the manuscript. This work was supported by NSF grants ACI 96-19019, AST 00-71019, AST 02-06299, and AST 03-07690, and NASA ATP grants NAG5-12140, NAG5-13292, and NAG5-13381.

## REFERENCES

- Barkana R., Loeb A. 2004, *ApJ*, 609, 474  
Barton E.J., Davé R., Smith J.-T., Papovich C., Hernquist L. Springel V. 2004, *ApJ*, 604, L1  
Becker R. H., et al. 2001, *AJ*, 122, 2850  
Bond J. R., Cole S., Efstathiou G., Kaiser N. 1991, *ApJ*, 379, 440  
Bromm V., Kudritzki R. P., Loeb A. 2001, *ApJ*, 552, 464  
Cen R. 2005, submitted to *ApJ* (astro-ph/0507014)  
Ciardi B., Stoehr F., White S. D. M. 2003, *MNRAS*, 343, 1101  
Cooray A., Sheth R. 2002, *Physics Reports*, 372, 1  
Fan X., et al. 2002, *AJ*, 123, 1247  
Furlanetto S. R., Hernquist L., Zaldarriaga M. 2004a, *MNRAS*, 354, 695 [FHZ04]  
Furlanetto S. R., McQuinn M., Hernquist L. 2005a, in preparation  
Furlanetto S. R., Oh S. P. 2005, in press at *MNRAS* (astro-ph/0505065)  
Furlanetto S. R., Schaye J., Springel V., Hernquist L. 2005b, *ApJ*, 622, 7  
Furlanetto S. R., Zaldarriaga M., Hernquist L. 2004b, *ApJ*, 613, 1 [FZH04]  
—. 2004c, *ApJ*, 613, 16  
Gunn J. E., Peterson B. A. 1965, *ApJ*, 142, 1633  
Haiman Z. 2002, *ApJ*, 576, L1  
Haiman Z., Cen R. 2005, *ApJ*, 623, 627  
Hamana T., Ouchi M., Shimasaku K., Kayo I., Suto Y. 2004, *MNRAS*, 347, 813  
Hernquist L., Springel V. 2003, *MNRAS*, 341, 1253  
Hu E. M., et al. 2002, *ApJ*, 568, L75  
Iliev I. T., Scannapieco E., Shapiro P. R. 2005, *ApJ*, 624, 491  
Kogut A., et al. 2003, *ApJS*, 148, 161  
Lacey C., Cole S. 1993, *MNRAS*, 262, 627  
Le Delliou M., Lacey C., Baugh C. M., Guiderdoni B., Bacon R., Courtois H., Sousbie T., Morris S. L., 2005a, *MNRAS*, 357, L11  
Le Delliou M., Lacey C. G., Baugh C. M., Morris S. L., 2005, submitted to *MNRAS* (astro-ph/0508186)  
Madau P., Rees M. J. 2000, *ApJ*, 542, L69  
Malhotra S., Rhoads J. E. 2004, *ApJ*, 617, L5  
McQuinn M., Furlanetto S. R., Hernquist L., Zahn O., Zaldarriaga M. 2005, *ApJ*, in press (astro-ph/0504189)  
Mesinger A., Haiman Z. 2004, *ApJ*, 611, L69  
Miralda-Escudé J. 1998, *ApJ*, 501, 15  
Miralda-Escudé J., Haehnelt M., Rees M. J. 2000, *ApJ*, 530, 1  
Mo H. J., White S. D. M. 1996, *MNRAS*, 282, 347  
Nagamine K., Springel V., Hernquist L., Machacek M. 2004a, *MNRAS*, 350, 385  
Nagamine K., Cen R., Hernquist L., Ostriker J., Springel V. 2004b, *ApJ*, 610, 45  
Night C., Nagamine K., Springel V., Hernquist L. 2005, *MNRAS*, submitted (astro-ph/0503631)  
Oh S. P., Furlanetto S. R. 2005, *ApJ*, 620, L9  
Ouchi M., et al. 2005, *ApJ*, 620, L1  
Partridge R. B., Peebles P. J. E. 1967, *ApJ*, 147, 868  
Press W. H., Schechter P. 1974, *ApJ*, 187, 425  
Rhoads J. E., et al. 2004, *ApJ*, 611, 59  
Santos M. R. 2004, *MNRAS*, 349, 1137  
Santos M. R., et al. 2004, *ApJ*, 606, 683  
Shapley A. E., Steidel C. C., Pettini M., Adelberger K. L. 2003, *ApJ*, 588, 65  
Sheth R. K. 1998, *MNRAS*, 300, 1057  
Sokasian A., Abel T., Hernquist L., Springel V. 2003, *MNRAS*, 344, 607  
Sokasian A., Yoshida N., Abel T., Hernquist L., Springel V. 2004, *MNRAS*, 350, 47  
Spergel D. N., et al. 2003, *ApJS*, 148, 175  
Springel V., Hernquist L. 2003, */mnras*, 339, 312  
Stanway E. R., et al. 2004, *ApJ*, 604, L13  
Stern D., Yost S. A., Eckart M. E., Harrison F. A., Helfand D. J., Djorgovski S. G., Malhotra S., Rhoads J. E. 2005, *ApJ*, 619, 12  
Taniguchi Y., et al. 2005, *PASJ*, 57, 165  
Theuns T., et al. 2002, *ApJ*, 567, L103  
White R. L., Becker R. H., Fan X., Strauss M. A. 2003, *AJ*, 126, 1  
Wyithe J. S. B., Loeb A. 2004a, *Nature*, 432, 194  
—. 2004b, *Nature*, 427, 815  
—. 2005, *ApJ*, 625, 1  
Zahn O., Zaldarriaga M., Hernquist L., McQuinn M. 2005, submitted to *ApJ* (astro-ph/0503166)  
Zaldarriaga M., Furlanetto S. R., Hernquist L. 2004, *ApJ*, 608, 622